

Citation for published version:
Aliev, GN, Amonkosolpan, J & Wolverson, D 2016, 'Observation of oxygen dimers via energy transfer from silicon nanoparticles', *Physical Chemistry Chemical Physics*, vol. 18, no. 2, pp. 690-693. https://doi.org/10.1039/c5cp04192a

10.1039/c5cp04192a

Publication date:

2016

Document Version Publisher's PDF, also known as Version of record

Link to publication

Publisher Rights CC BY CC-BY

University of Bath

Alternative formats

If you require this document in an alternative format, please contact: openaccess@bath.ac.uk

General rights

Copyright and moral rights for the publications made accessible in the public portal are retained by the authors and/or other copyright owners and it is a condition of accessing publications that users recognise and abide by the legal requirements associated with these rights.

If you believe that this document breaches copyright please contact us providing details, and we will remove access to the work immediately and investigate your claim.

Download date: 07. Mar. 2023

PCCP



COMMUNICATION

View Article Online



Observation of oxygen dimers via energy transfer from silicon nanoparticles†

Cite this: DOI: 10.1039/c5cp04192a

Gazi N. Aliev, a Jamaree Amonkosolpan and Daniel Wolverson*

Received 17th July 2015, Accepted 30th November 2015

DOI: 10.1039/c5cp04192a

www.rsc.org/pccp

Energy transfer from photo-excited excitons confined in silicon nanoparticles to oxygen dimers adsorbed on the nanoparticle surfaces is studied as a function of temperature and magnetic field. Quenching features in the nanoparticle photoluminescence spectrum arise from energy transfer to the oxygen dimers with and without the emission of Si $\mathsf{TO}(\Delta)$ phonons and, also, with and without the vibrational excitation of the dimers. The dependence of the quenching on magnetic field shows that energy transfer is fast when a dimer is present, allowing an estimate of the proportion of the nanoparticles with adsorbed dimers.

Semiconducting or metallic nanoparticles offer numerous ways of manipulating the light-matter interaction, and offer huge potential in areas as diverse as plasmonics, sensing, photocatalysis, quantum cryptography, nanoscale electronics, and also imaging, diagnostic, and therapeutic uses in medicine. In the context of biomedical applications, silicon nanoparticles (SiNPs) are promising due to their good biocompatibility, since Si is metabolized rapidly to benign end-products. E-5

SiNPs within porous silicon have size-dependent optical transition energies which can be tuned over the visible spectrum. The photo-excitation of large SiNPs with weak quantum confinement generates indirect excitons with long lifetimes and a high probability of interaction with nearby molecules. One well-known example is the direct electron exchange-controlled (Dexter-type) energy transfer from photo-excited SiNPs to isolated oxygen molecules in the ground triplet state $^3\Sigma$, exciting these to the $^1\Sigma$ singlet state. Singlet $^{9-11}$ Singlet $^{1}O_2$ is highly reactive, and can initiate cellular apoptosis, leading to possible applications in photo-dynamic cancer therapy. Singlet $^{12-14}$ Fig. 1 shows the reversible quenching of SiNP photoluminescence (PL) by adsorbed O_2 that can be used to monitor these energy transfer processes. In Fig. 1, the broad PL band is made up of emission

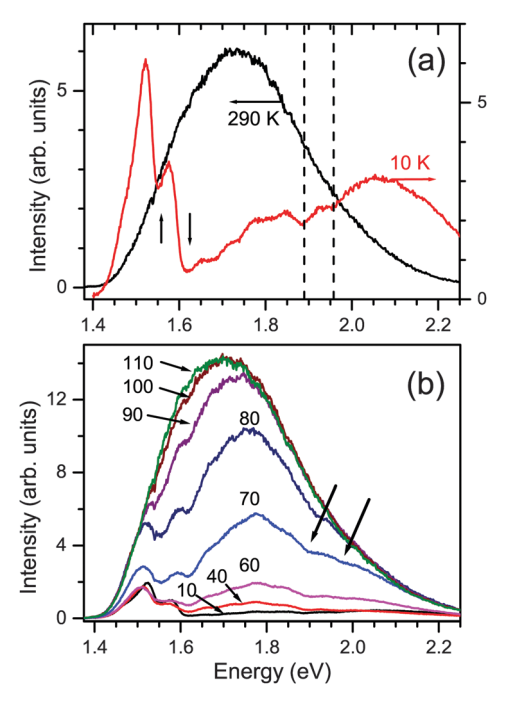


Fig. 1 (a) Photoluminescence (PL) spectra of a silicon nanoparticle assembly at 10 K with a high level of adsorbed O_2 (red curve) and at 290 K without O_2 present (black curve). The vertical arrows indicate two PL quenching lines due to isolated oxygen molecules and the dashed lines indicate two spectral features arising from O_2 dimers; the spectra are normalised to the same peak height. (b) PL spectra of the same sample with high adsorbed O_2 concentration as a function of temperature increasing from 10 K to 110 K; arrows show the features arising from O_2 dimers.

by a highly disperse ensemble of SiNPs in porous silicon ranging from weak to strong quantum confinement, thus providing donors over a wide energy range. With increasing confinement, there is a gradual transition from phonon-assisted to no-phonon $PL^{7,8,15,16}$ with a rapid decrease in exciton lifetime, and so the probability of energy transfer declines. By comparison with many previous studies, the PL of Fig. 1 is typical of porous silicon and is consistent with a distribution of sizes from $\sim 2-9$ nm, peaked at ~ 3.5 nm. $^{8,17-22}$

^a Department of Physics, University of Bath, Bath, BA2 7AY, UK. E-mail: d.wolverson@bath.ac.uk; Tel: +44-{0}1225-383321

^b Department of Physics, Srinakharinwirot University, Bangkok 10110, Thailand

[†] Data supporting this study are available from the University of Bath data archive. See DOI: 10.15125/BATH-00119

Communication

Besides O2, energy transfer from SiNPs to adsorbed organic molecules has been demonstrated, including anthracene, naphthalene, β -carotene and fullerenes;²³ in contrast to O_2 , these possess a singlet ground state and triplet first excited state. Analysis of the partially-quenched PL spectrum of an ensemble of SiNPs revealed the molecular singlet-triplet splitting Δ_{ST} , so that one can regard the energy transfer process from SiNPs as a spectroscopic tool for probing the excited states of adsorbates.²³ Here, we consider one special example of this, the excitation of adsorbed oxygen dimers (or "dimols") (2O2), which gives rise to the features marked in Fig. 1(b). Similar features were reported earlier^{24,25} but tests of the dimer model have been lacking, and its dependence on spin selection rules has not been investigated. We have used magneto-PL measurements at low temperatures and obtain unusually clear signatures of energy transfer to 2O2.

Magneto-PL measurements were carried out in liquid He $(T \sim 1.5 \text{ K})$ in a superconducting magnet providing a field B of up to 6 T into which gaseous O2 could be condensed on the cold SiNPs; the sample could be heated and pumped to remove the oxygen. PL measurements in zero field were carried out in a closed cycle cryostat ($T \ge 10$ K) with the same capability of adding and removing O2. SiNPs were produced by electrochemical etching of p-type boron-doped silicon wafers and the nanoparticles were left supported within a porous etched layer of thickness $\sim 8 \mu m$. The SiNP surface was exposed to air before measurements; by FTIR, we find surfaces treated this way to be substantially Si-H terminated but partially oxidised, by reference to characterization reviews. 6 Details of the etching and resulting porosity are given elsewhere.²⁶ PL from the SiNPs was excited by a continuous wave (CW) solid state laser (~ 450 nm, power ~ 0.5 mW over area ~ 1 mm²) and PL from 2O2 was excited using a mode-locked Yb-doped fiber laser (\sim 1064 nm, repetition rate 20 MHz, average CW power \sim 2-3 W); PL was detected using a response-corrected spectrometer (Acton SpectroPro 2300i) and cooled CCD.

In Fig. 1(a), we show the PL spectra of a porous Si layer at 290 K in the absence of O2; the PL curve is featureless, showing that the dips that appear after O2 exposure are not artefacts of the detection system. Oxygen was then adsorbed on the same layer at 10 K; earlier estimates based on similar PL spectra suggested an average of 7-8 O₂ molecules per SiNP.²⁷ Fig. 1(a) shows the PL is strongly quenched by energy transfer above the threshold energy 1.63 eV which corresponds²⁸ to the isolated O₂ triplet-singlet transition $^3\Sigma$ to $^1\Sigma$. SiNPs emitting PL below this energy are less effectively quenched but the involvement of phonons in the PL emission produces a relatively sharp dip in the PL near 1.57 eV.²⁷ All spectral features present in Fig. 1 are quenching bands; for example, the prominent peak near 1.5 eV is simply the residual part of the PL spectrum for SiNPs lying below the $^3\Sigma$ to $^1\Sigma$ threshold. As T is increased for the same sample with high O2 coverage, Fig. 1(b) shows that the PL intensity recovers to a featureless spectrum by around 100 K due to desorption of the O2. A new feature is the small dip in the PL spectra near 1.95 eV up to $T \sim 80$ K which suggests the presence of $2O_2$ dimers, for which the $2(^1\Delta) \rightarrow 2(^3\Sigma)$ fluorescence

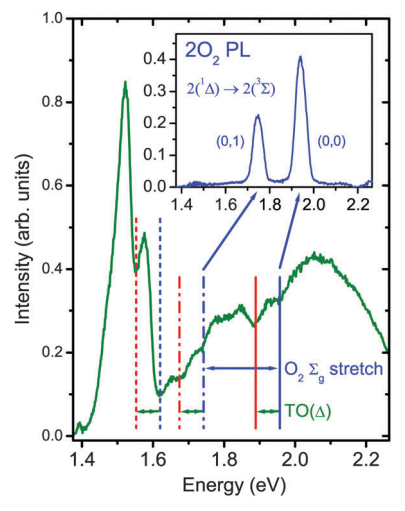


Fig. 2 Silicon nanoparticle photoluminescence (PL) at 10 K strongly quenched by adsorbed oxygen, showing quenching features due to oxygen dimers (vertical solid blue line) and phonon replicas (vertical solid red line and dash-dotted lines). Also shown is the quenching feature due to single oxygen molecules (blue dotted line) and its phonon replica (red dotted line). Inset: The low temperature PL of oxygen dimers under pulsed excitation, with the final vibrational quantum states indicated

transition is at twice the energy of the $^{1}\Delta \rightarrow ^{3}\Sigma$ transition of O₂ (0.98 eV).28

Charge transfer to the adsorbed oxygen will also quench the PL but does not introduce sharp spectral features²⁹⁻³² and is impeded by any surface oxide layer. On the other hand, surface oxides may introduce silica-related defect states that can contribute to the observed PL particularly at higher energies (e.g., the "blue band" at ~ 2.5 eV);¹⁹ in this spectral region, the sensitivity of PL to O2 is seen to reduce. Dangling bonds, however, act as non-radiative recombination centres8 so that affected SiNPs will be undetected in PL. The present quenching bands affect luminescent SiNPs, are at lower energies than the blue band (\leq 1.9 eV) and show silicon $TO(\Delta)$ phonon replicas, so we rule out charge transfer and common defect states as explanations for these features.

Fig. 2 shows a PL spectrum of a SiNP sample with a high oxygen concentration to display the $2(^{1}\Delta) \rightarrow 2(^{3}\Sigma)$ transition more clearly (marked by the solid blue vertical line), together with various replicas of this band which we discuss in the following. In the inset to Fig. 2, we show the luminescence spectrum of oxygen from this sample, excited using pulsed excitation.28 The two optical transitions of oxygen dimers at 1.95 and 1.75 eV are clearly seen (weak signals necessitated the low spectral resolution). The higher energy PL band is due to the $2(^{1}\Delta) \rightarrow 2(^{3}\Sigma)$ transition and the lower band arises from the same electronic transition but with an increase in the vibrational quantum number of the dimer (energy of the O2 stretch is \sim 192 meV). The detection of these signals is a direct proof of the presence of oxygen dimers, since isolated oxygen molecules do not show PL at these energies. This supports earlier assignments²⁷ of the dip in the PL spectra to 2O₂ dimers; however, if only this dip is detected, it is not possible to conclude whether it arises trivially from optical absorption of the SiNP PL (e.g., by an intervening layer of oxygen dimers) or whether it is due to

PCCP

directly on the nanoparticle.

energy transfer from a SiNP exciton to an oxygen dimer adsorbed

Consideration of the data of Fig. 2, however, shows that the latter interpretation is correct. Two more strong dips appear in the SiNP PL signal, centered at 1.89 eV and 1.68 eV. These are thus located at energy shifts of around 60 meV below the respective dimer absorption bands. This is similar to the behavior of the dip at 1.63 eV due to quenching of the PL by triplet–triplet Dexter-type energy transfer to isolated O₂ molecules, which appears in conjunction with a second dip at 1.57 eV. The resemblance is strong; for all of the quenching bands at 1.63 eV (isolated O₂) and at 1.75 eV and 1.95 eV (oxygen dimers) their lower-energy phonon replicas are as strong, or even stronger, than the quenching bands themselves.

This can be explained in terms of the indirect bandgap of silicon; quantum confinement effects in the SiNPs relax the momentum conservation requirements for radiative exciton recombination but not completely, so that phonon-assisted PL is still significant even for nanoparticles small enough that quantum confinement shifts give PL energies around 1.9 eV.7,8,15,16 Therefore, the SiNP PL band near the dimer transition energy must be attributed at least in part to momentum-conserving $TO(\Delta)$ -assisted exciton recombination. Two distinct sets of nanoparticles then dominate the transfer of exciton energy to a given adsorbate molecule: those (type A) whose exciton energy equals the adsorbate transition energy and those (type B) whose exciton energy is higher by a $TO(\Delta)$ phonon energy (57 meV), so that energy transfer is accompanied by $TO(\Delta)$ emission.²⁷ Thus, if nanoparticles of type A are quenched by energy transfer, a dip in the PL spectrum appears one $TO(\Delta)$ phonon energy below the adsorbate energy, whereas the dip located at the adsorbate energy arises from the quenching of higher energy SiNPs of type B.

In this model, we can also understand the difference in depth of the two dips of each pair in the PL spectrum. Firstly, the fundamental rates of transfer processes from SiNPs of type A and type B are not necessarily equal, since only the higher energy dip requires phonon-assisted emission. Secondly, those SiNPs emitting at the lower energy (type A) are larger than those of type B and thus have a potentially higher adsorbate coverage, higher net transfer probability, and deeper dip in the PL spectrum. If we model the SiNPs as spherical particles, we can use a proposed quantitative correlation between diameter and exciton energy³³ to estimate the increase in surface area from particles of type B to those of type A; we find increases of 11% (for \sim 3 nm diameter particles with exciton energies near 1.95 eV) to 18% (\sim 4.5 nm, 1.63 eV). For the high oxygen coverages discussed earlier, changes in surface area of this magnitude lead to one additional O2 molecule on average being located on type A particles than on type B, and thus a stronger quenching dip for type A particles at the lower energy of each pair. Even for more realistic models of the SiNP shape, a correlation between surface area and exciton energy will still exist.²²

The observation of the replica at 1.89 eV of the dimer quenching band at 1.95 eV is crucial here because it gives a demonstration that energy transfer is the origin of the dimerrelated features: simple optical absorption of the SiNP PL by

oxygen dimers would give absorption bands only at the two dimer transition energies, with no phonon-assisted replicas. This result may also lead to the re-interpretation of spectral features that have sometimes been ascribed to energy transfer to isolated O₂ *via* multi-phonon processes. Here all features of Fig. 2 are interpreted in terms of single- or no-phonon transfer processes. A phonon replica of one dimer band was identified in a previous report in time-resolved PL spectra²⁹ but its significance (allowing one to discount direct optical absorption by oxygen dimers) was not discussed. We believe the present data represents the first direct observation of this band in a CW experiment; furthermore, we also see energy transfer to dimers at 1.75 eV, which shows for the first time a vibrational signature of an adsorbate in the SiNP quenching spectrum.

Finally, we consider the dependence of the SiNP:O2 PL spectra on magnetic field at low T. We showed elsewhere that the PL recovers as the magnetic field lifts the spin degeneracies of the exciton and oxygen triplet levels and thereby suppresses the quenching by isolated O₂ due to triplet-triplet transfer.²⁶ This is evident in Fig. 3(a), which shows that the PL recovers dramatically in intensity as the magnetic field increases from zero to 6 T; this magnetic field dependence establishes that the donor state for energy transfer to isolated O2 is a triplet exciton, and implies that the same is true for the dimers. Fig. 3(b) presents the same data but normalized to the zero field spectrum. It is striking in Fig. 3(b) that the features due to dimers are absent after this normalization; thus, energy transfer to dimers accounts for a constant (field-independent) fraction of the PL. This can be understood if a constant proportion of the SiNPs have adsorbed dimers (as well as isolated O2 molecules) and that the spin-conserving energy transfer to the dimers competes with transfer to isolated O2, as suggested by time-resolved studies. 29 The total depth of the dimer-related dips in the PL at 1.89 and 1.95 eV

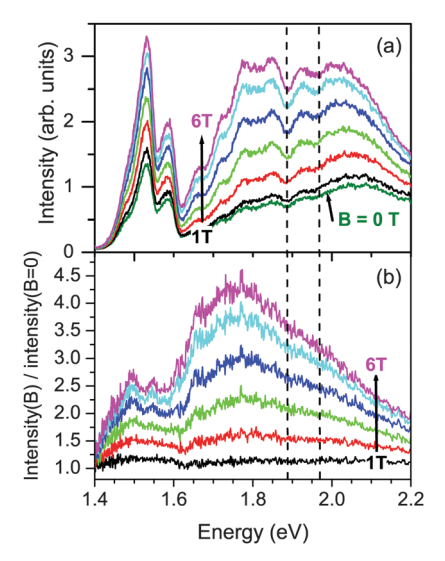


Fig. 3 (a) Photoluminescence spectra at 1.5 K of silicon nanoparticles with a high level of adsorbed oxygen for magnetic fields from zero to 6 Tesla; (b) the spectra of part (a) from 1 Tesla to 6 Tesla, normalized to the spectrum at zero field. The dashed lines indicate the expected energy positions of the quenching bands due to energy transfer to oxygen dimers.

in Fig. 3(a) is about 16% of the PL intensity at nearby energies and this is a direct measure of the proportion of SiNPs that have an adsorbed dimer available for energy transfer; thus, about 16% of the relevant SiNPs have one or more adsorbed dimers under the conditions of this particular experiment. By contrast, the rate of energy transfer to isolated O_2 is field-dependent so that its quenching features do not disappear on normalization, as seen in Fig. 3(b).

In summary, energy transfer takes place from photoexcited excitons in silicon nanoparticles to oxygen dimers adsorbed on the nanoparticle surfaces at low temperatures; phonon replicas of the PL quenching features demonstrate that this is due to resonant energy transfer from quantum confined SiNP excitons rather than *via* optical emission and absorption. These quenching bands reflect not only the electronic but also the vibrational energy levels of the adsorbed oxygen dimers. Finally, the process of energy transfer to oxygen dimers is found to be fast and independent of magnetic field.

Acknowledgements

Work was supported by the Engineering and Physical Sciences Research Council, UK, grant EP/J007552/1. We thank James Stone for his help with the pulsed excitation measurements and J. John Davies and Bernhard Goller for useful discussions.

References

- 1 N. T. K. Thanh and L. A. W. Green, *Nano Today*, 2010, 5, 213–230.
- 2 J.-H. Park, L. Gu, G. von Maltzahn, E. Ruoslahti, S. N. Bhatia and M. J. Sailor, *Nat. Mater.*, 2009, **8**, 331–336.
- 3 H. A. Santos, J. Riikonen, J. Salonen, E. Makila, T. Heikkila, T. Laaksonen, L. Peltonen, V.-P. Lehto and J. Hirvonen, *Acta Biomater.*, 2010, **6**, 2721–2731.
- 4 L. M. Bimbo, M. Sarparanta, H. A. Santos, A. J. Airaksinen, E. Mkil, T. Laaksonen, L. Peltonen, V.-P. Lehto, J. Hirvonen and J. Salonen, *ACS Nano*, 2010, 4, 3023–3032.
- 5 L. A. Osminkina, V. A. Sivakov, G. A. Mysov, V. A. Georgobiani, U. Natashina, F. Talkenberg, V. V. Solovyev, A. A. Kudryavtsev and V. Y. Timoshenko, *Nanoscale Res. Lett.*, 2014, 9, 463.
- 6 M. J. Sailor, *Porous Silicon in Practice: Preparation, Characterization and Applications*, Wiley-VCH, Weinheim, 2011.
- 7 D. Kovalev, H. Heckler, M. Ben-Chorin, G. Polisski, M. Schwartzkopff and F. Koch, *Phys. Rev. Lett.*, 1998, 81, 2803–2806.
- 8 V. A. Belyakov, V. A. Burdov, R. Lockwood and A. Meldrum, Adv. Opt. Technol., 2008, 2008, 32.
- 9 D. Kovalev, E. Gross, N. Knzner, F. Koch, V. Y. Timoshenko and M. Fujii, *Phys. Rev. Lett.*, 2002, **89**, 137401.
- 10 M. Fujii, S. Minobe, M. Usui, S. Hayashi, E. Gross, J. Diener and D. Kovalev, *Phys. Rev. B: Condens. Matter Mater. Phys.*, 2004, **70**, 085311.

- 11 E. Gross, D. Kovalev, N. Kunzner, J. Diener and F. Koch, *Quantum Dots*, 2004, **789**, 17–22.
- 12 V. Y. Timoshenko, A. A. Kudryavtsev, L. A. Osminkina, A. S. Vorontsov, Y. V. Ryabchikov, I. A. Belogorokhov, D. Kovalev and P. K. Kashkarov, *JETP Lett.*, 2006, 83, 423–426.
- 13 C. Lee, H. Kim, Y. Cho and W. I. Lee, *J. Mater. Chem.*, 2007, 17, 2648–2653.
- 14 L. Xiao, L. Gu, S. B. Howell and M. J. Sailor, ACS Nano, 2011, 5, 3651–3659.
- 15 P. Calcott, K. Nash, L. Canham, M. Kane and D. Brumhead, J. Lumin., 1993, 57, 257–269.
- 16 D. Kovalev, H. Heckler, B. Averboukh, M. Ben-Chorin, M. Schwartzkopff and F. Koch, *Phys. Rev. B: Condens. Matter Mater. Phys.*, 1998, 57, 3741–3744.
- 17 D. Kovalev, H. Heckler, G. Polisski and F. Koch, *Phys. Status Solidi B*, 1999, **215**, 871–932.
- 18 G. Ledoux, O. Guillois, D. Porterat, C. Reynaud, F. Huisken, B. Kohn and V. Paillard, *Phys. Rev. B: Condens. Matter Mater. Phys.*, 2000, **62**, 15942–15951.
- 19 O. Bisi, S. Ossicini and L. Pavesi, Surf. Sci. Rep., 2000, 38, 1–126.
- 20 F. Huisken, G. Ledoux, O. Guillois and C. Reynaud, *Adv. Mater.*, 2002, **14**, 1861–1865.
- 21 M. B. Gongalsky, A. Y. Kharin, S. A. Zagorodskikh, L. A. Osminkina and V. Y. Timoshenko, *J. Appl. Phys.*, 2011, **110**, 013707.
- 22 R. Ghosh, P. K. Giri, K. Imakita and M. Fujii, Nanotechnology, 2014, 25, 045703.
- 23 B. Goller, S. Polisski and D. Kovalev, *Phys. Rev. B: Condens. Matter Mater. Phys.*, 2007, 75, 073403.
- 24 D. Kovalev and M. Fujii, Adv. Mater., 2005, 17, 2531-2544.
- 25 B. Goller, S. Polisski, H. Wiggers and D. Kovalev, *Appl. Phys. Lett.*, 2010, **96**, 211901.
- 26 J. Amonkosolpan, G. N. Aliev, D. Wolverson, P. A. Snow and J. J. Davies, *Nanoscale Res. Lett.*, 2014, 9, 342.
- 27 E. Gross, D. Kovalev, N. Kunzner, J. Diener, F. Koch, V. Y. Timoshenko and M. Fujii, *Phys. Rev. B: Condens. Matter Mater. Phys.*, 2003, **68**, 115405.
- 28 A. Yamagishi, T. Ohta, J. Konno and H. Inaba, *J. Opt. Soc. Am.*, 1981, 71, 1197–1201.
- 29 M. Fujii, D. Kovalev, B. Goller, S. Minobe, S. Hayashi and V. Y. Timoshenko, *Phys. Rev. B: Condens. Matter Mater. Phys.*, 2005, **72**, 165321.
- 30 G. Di Francia, L. Quercia, I. Rea, P. Maddalena and S. Lettieri, *Sens. Actuators, B*, 2005, **111**, 117–124.
- 31 N. Liu, M.-M. Shi, X.-W. Pan, W.-M. Qiu, J.-H. Zhu, H.-P. He, H.-Z. Chen and M. Wang, J. Phys. Chem. C, 2008, 112, 15865–15869.
- 32 B. H. Meekins, Y.-C. Lin, J. S. Manser, K. Manukyan, A. S. Mukasyan, P. V. Kamat and P. J. McGinn, *ACS Appl. Mater. Interfaces*, 2013, 5, 2943–2951.
- 33 C. Delerue, G. Allan and M. Lannoo, *Phys. Rev. B: Condens. Matter Mater. Phys.*, 1993, **48**, 11024–11036.